PROCEEDINGS OF SCIENCE

Complex potential at $T > 0$ from fine lattices

Gaurang Parkar[b,*] **and Olaf Kaczmarek**[a], **Rasmus Larsen**[b], **Swagato Mukherjee**[c], **Peter Petreczky**[c], **Alexander Rothkopf**[b], **Johannes Heinrich Weber**[d]

[a] *Fakultät für Physik, Universität Bielefeld, D-33615 Bielefeld, Germany*
[b] *Faculty of Science and Technology, University of Stavanger, NO-4036 Stavanger, Norway,*
[c] *Physics Department, Brookhaven National Laboratory, Upton, New York 11973, USA*
[d] *Institut für Physik & IRIS Adlershof, Humboldt-Universität zu Berlin, D-12489 Berlin, Germany*

E-mail: gaurang.parkar@uis.no

We study the Wilson line correlation function in Coulomb gauge on lattices in 2+1 flavor QCD with the aim to determine the complex potential at non-zero temperature and present past results on coarse lattices along with some preliminary results on newly generated fine lattices. From the analysis of the Wilson line correlation function after the subtraction of a temperature independent UV part we conclude that the corresponding spectral function is well described by a dominant peak. If a potential interpretation is applicable, the peak position and effective width correspond to the potential's real and imaginary parts. We positively confirm this potential interpretation with a peak position that is temperature independent and shows no sign of screening, while the peak width shows a strong temperature dependence.

The 39th International Symposium on Lattice Field Theory, LATTICE2022 8th-13th August, 2022 Bonn

*Speaker

PoS(LATTICE2022)188

1. Introduction

The bound states of quark and anti-quark pair (quarkonia) have been of great interest in heavy ion collisions since the work by Matsui and Satz [1]. An understanding of these bound states holds key to probing the existence of quark gluon plasma in heavy ion collisions.

There is a separation of scales $M \gg Mv \gg Mv^2$ and $M \gg \Lambda_{QCD}$ (M is the heavy quark mass and v is the relative velocity) present, thus we can integrate out the hard scale M leading to a theory of non-relativistic QCD (NRQCD). We can further restrict our focus on the ultrasoft scale Mv^2. A new effective field theory called potential NRQCD (pNRQCD) now emerges, which is a theory of colour singlet and octet heavy meson fields. The potential appears as a parameter (Wilson coefficient) of this effective field theory. At zero temperature, applicability of a potential picture has been confirmed [2], and affirmatively compared to perturbative predictions [3]. Our goal now is to establish whether such a potential exists at $T \neq 0$ and if it does what is the form of such a potential.

The real-time Wilson loop describes the time evolution of the static quark-antiquark pair. We cannot directly access the real-time Wilson loop on the lattice since simulations in lattice QCD are done in imaginary time. Thus we make use of the concept of the spectral function, which can be interpreted as a link between the real and imaginary time physics of the spectral function [4]

$$W_{\square}(r,t) = \int d\omega e^{-i\omega t}\rho_{\square}(r,\omega) \leftrightarrow \int d\omega e^{-\omega\tau}\rho_{\square}(r,\omega) = W_{\square}(r,\tau). \tag{1}$$

In order to extract the spectral function we must invert the right hand side of equation 1. However, in practice the presence of only a few noisy data points renders the problem ill-posed. In hard thermal loop perturbation theory we get a dominant peak in the spectral function [5], which can be related to a potential with a screened real-part and a finite imaginary part [6].

The goal for this proceedings to compare results on the spectral structure of the Wilson loop on coarse HISQ lattices and show some preliminary results on the newly generated fine lattices. A previous comparison using a more restricted dataset on fine lattices, small differences in the UV subtraction, and HYP smearing [7] instead of gradient flow [8, 9] had led to qualitatively similar conclusions [10].

2. Results on coarse HISQ lattices

We performed calculations on Wilson loop and Wilson line correlators in Coulomb gauge from (2+1)-flavour QCD configurations generated from HOTQCD and TUMQCD. The Highly Improved Staggered Quark (HISQ) action was used to generate $2 - 6 \times 10^4$ configurations to make sure that we have high enough statistics. We use the Wilson line correlator instead of Wilson loop because it helps simplifying the analysis. While changing from the Wilson loop to Wilson line correlator would introduce some changes in the amplitude of the spectral function, the position and width of the dominant peak should remain unchanged. It has been argued in leading order HTL perturbation theory that the position and lowest lying peak does not change when switching from Wilson loop to Wilson line [5]. The Wilson line correlator is defined as,

$$W(r,\tau,T) = \frac{1}{3}\langle Tr(L(0,\tau)L^{\dagger}(r,\tau))\rangle_T \tag{2}$$

where $L(r,\tau) = \exp(\int_0^\tau A_4(r,\tau')d\tau')$. $N_\sigma \times N_\tau$ lattices were used with $N_\tau = 10, 12, 16$ keeping the ratio $N_\sigma/N_\tau = 4$ fixed. The fixed box approach was used spanning a temperature of 140 MeV to 2 GeV. For high temperatures ($T > 300$ MeV) the light quark (u and d) mass was set for some ensembles to $m_s/5$; otherwise it was set to $m_s/20$. We present four different methods of analysis in this proceeding. For a more detailed overview of the methods refer to [11].

We first compute cumulants of the correlation function and compare it with HTL (hard thermal loop) perturbation theory. We define the first cumulant as effective mass :

$$m_{eff}(\tau) = -\partial_\tau \ln W(\tau) \tag{3}$$

We carried out the subtraction procedure as done in [12] where the UV part of the correlator is subtracted using the $T = 0$ correlator. In figure 1 we show the difference of effective masses of the subtracted correlator and singlet free energies. We observed that HTL does not quantitatively fit the data except for some specific temperature and some specific separation distance.

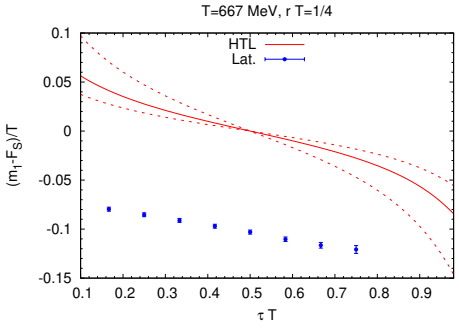

Figure 1: The figure shows effective mass subtracted from free energies at $T = 667$ The solid lines in red show the HTL result for renormalisation scale $\mu = 2\pi T$ and the dashed lines represent variation of the scale by a factor of two.

From the cumulant analysis we found that we can only extract the first and the second cumulant from the correlator data. The lattice data is sensitive only to the peak position Ω and the effective width Γ. We can thus parameterise the UV subtracted correlator as :

$$C_{sub}(r,t) \approx \exp(-\Omega\tau + \frac{1}{2}\Gamma^2\tau^2 + O(\tau^3)) \tag{4}$$

This results in a Gaussian spectral function plus an addition term

$$\rho(\omega,T) = A(T)\exp(-\frac{|\omega - \Omega(T)|^2}{2\Gamma(T)^2}) + A^{cut}(T)\delta(\omega - \omega^{cut}(T)) \tag{5}$$

This ansatz ignores the tail on the high ω side of the peak and therefore is not completely consistent. However, the contribution of the high ω tail is exponentially suppressed by the kernel and therefore, the corresponding contribution to the correlation functions is very small and can be neglected at present level of statistical accuracy. The results after carrying out the Gaussian fits are shown in fig. 2.

The second method of analysis was the Padé interpolation. Historically, the Padé interpolation has not been used for spectral reconstruction as it requires high statistics. In this method we first

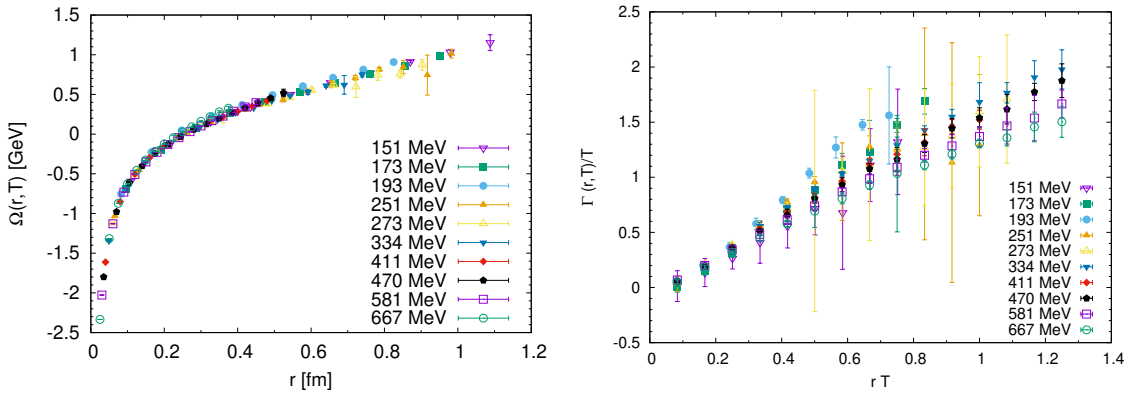

Figure 2: The peak position of the spectral function (Ω) and the (effective) width (Γ) as function of the separation obtained from Gaussian fits of the $N_\tau = 12$ lattices.

transform the Euclidean correlator into Matsubara frequency space. We then implement Padé interpolation in the form of continued fraction according to the Schlessinger prescription [13]. This is interpolation and not fitting and it avoids the problem of costly minimisation. An example of interpolated data is shown in fig. 3. Once we have the interpolated rational function we can obtain the pole structure of the correlator. The peak position and width are the real and imaginary parts of the dominant pole of the correlator. Results from Padé interpolation are shown in figure 4.

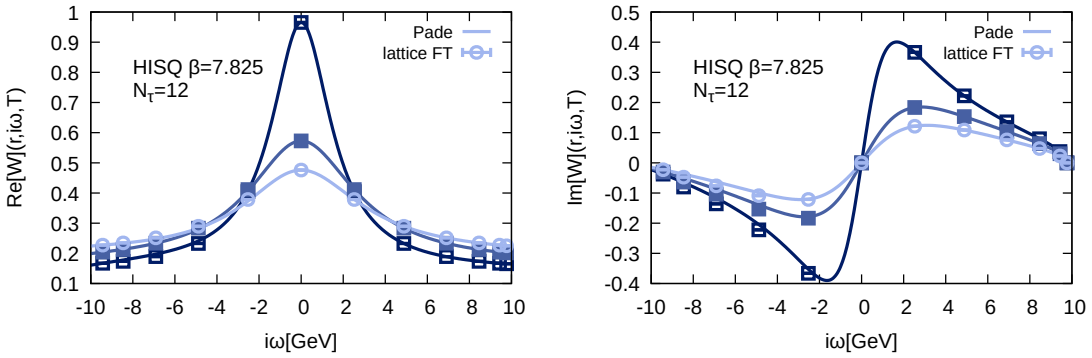

Figure 3: Discrete Fourier transform of the $T > 0$ Wilson line correlators at $T = 407$MeV ($\beta = 7.825$, $N_\tau = 12$) at spatial separation distances $r = 0.03872$ fm, $r = 0.1758$ fm and $r = 0.2964$ fm. The figure on the right shows the imaginary part and the one on the left shows the real part.

The third method applied was the Bayesian reconstruction using the BR method [14]. Unlike the Padé, Bayesian methods are designed to reproduce the Euclidean data and rely on the positive definiteness of the spectral function. However, for this study the Bayesian analysis fails at high temperatures as we saw non-monotonic behaviour of effective masses at small τ; which is manifestation of a non-positive spectral function. Such non-monotonous behaviour of effective masses is a feature of improved actions and has also been previously observed in [3]. We have thus only shown results at low temperature for the BR method.

The last method employed was the hard thermal loop inspired fits. It uses symmetry properties of thermal correlation functions of static quarkonia to extract a thermal potential for quarkonia using

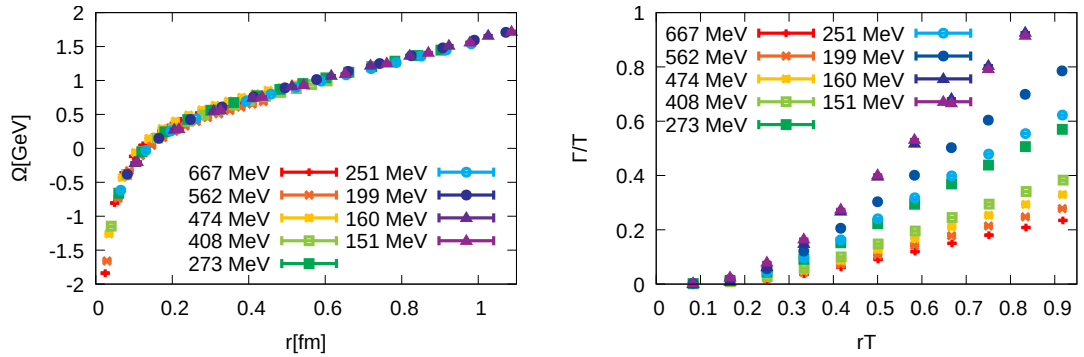

Figure 4: The peak position Ω and width Γ obtained from Padé interpolation for $N_\tau = 12$ lattices as a function of separation distance at different temperatures are shown in the figure above.

Euclidean Wilson loop data [15]. Results from this method are shown in fig 5.

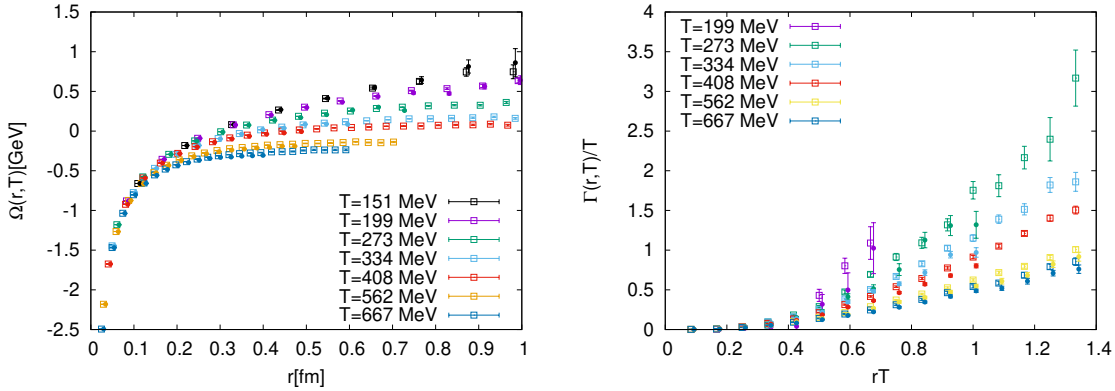

Figure 5: The peak position (Ω) and the width (Γ) from the HTL inspired method as function of separation distance at different temperatures.

We show a comparison of all methods in fig 6. The results from the Padé and model fits suggest that the peak position of the spectral function is independent of temperature. This result is indeed puzzling.

3. Preliminary results on Fine Lattices

Wilson line correlators were measured from configurations generated using the SIMULATeQCD [16, 17] code, and HISQ action was used to generate the ensembles. The light quark mass was set to $m_s/5$. $N_\sigma^3 \times N_\tau$ lattices were used with $N_\sigma = 96$ and $N_\tau = 20, 24, 28, 32, 56$. The pion mass is 310 MeV and lattice spacing $1/a = 7.1$ GeV. While analysing the correlators we found that the UV noise was very large at large τ, which would make the analysis rather challenging. Gradient flow [8, 9] was used as smearing to reduce this UV noise. More precisely we used Zeuthen flow [18]. 4D smearing comes at the cost of affecting the correlator at small τ and small distances (see fig. 7). Because we expect the small τ (large frequency) behavior to be temperature independent, it provides access to the relevant IR physics without too many losses. However, we do expect there

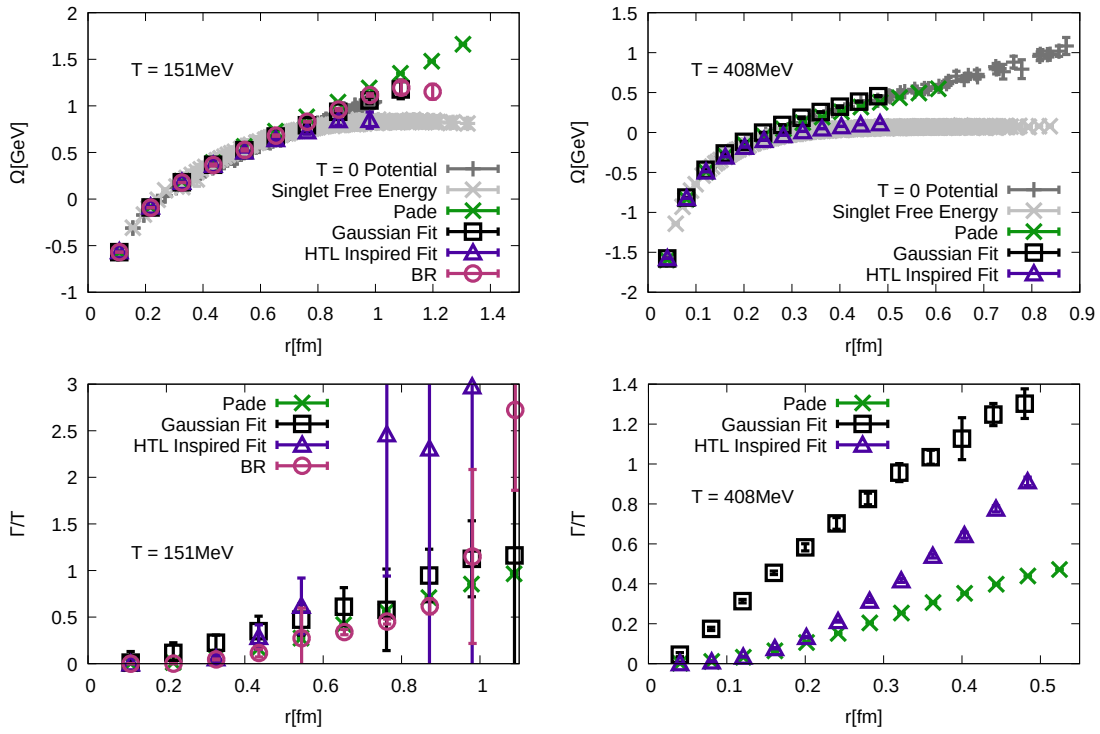

Figure 6: A comparison of the peak position (Ω) and width (Γ) obtained from different methods as a function of separation distance at temperatures 151 MeV and 408 MeV.

to be a significant change in the real part of the potential at small separation distances. These finer lattices should help us in improving resolution for spectral reconstruction in different methods.

We show some preliminary results using Gaussian fits for the new lattices in figures 8. The Gaussian fits show no significant change in the real part of the potential with changing temperature. This is consistent with results from the previous study with $N_\sigma = 48$ lattices. As expected we also see that smearing affects the peak position at small distances and it also shift it be a constant that has been removed by setting $\Omega = 0$ at $r/a = 3$. The effective width of the spectral function scales linearly with the temperature and rises almost linearly with the distance.

4. Conclusions

We have seen that the lowest feature of spectral functions of thermal Wilson Line correlators can be interpreted as encoding information about the real and imaginary part of a potential. From the different methods of analysis we see that the peak position and width of the spectral function highly depends on the method of analysis used since each of these methods is based on a different set of assumptions. This shows that the data are susceptible to multiple hypotheses. Results from Padé and Gaussian fits on coarse lattices and preliminary results on fine lattices show that the peak position of the spectral function is independent of temperature. These results are very puzzling indeed as they differ from some earlier studies in quenched QCD [15, 19] or even in full QCD [20]. Attempts to use Padé interpolation and improving Gaussian fits on fine lattices are still work in progress.

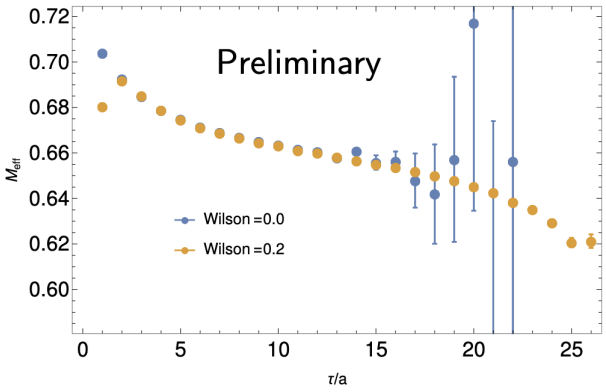

Figure 7: Effective masses for smeared vs unsmeared correlator for $N_\tau = 28$ lattices. We can see that the fluctuations at large τ diminish when smearing is applied.

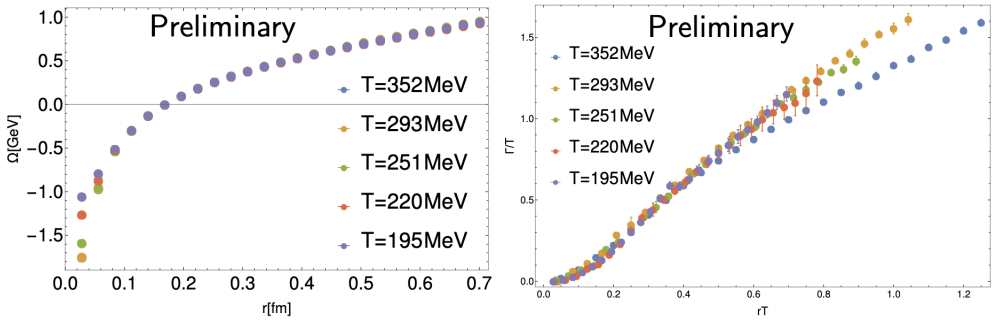

Figure 8: Preliminary results of peak position (Ω) and width (Γ) as a function of separation distances at different temperatures. The shifts introduced by different smearings at different temperatures are removed by setting $\Omega = 0$ for $r/a = 3$.

Acknowledgements

This material is based upon work supported by the U.S. Department of Energy, Office of Science, Office of Nuclear Physics through the (i) Contract No. DE-SC0012704, (ii) Scientific Discovery through Advance Computing (SciDAC) award *Fundamental Nuclear Physics at the Exascale and Beyond*, and (iii) Topical Collaboration in Nuclear Theory award *Heavy-Flavor Theory (HEFTY) for QCD Matter*. (iv) R.L., G.P. and A.R. are funded by the Research Council of Norway under the FRIPRO Young Research Talent grant 286883 with computing time provided by the PRACE award on JUWELS at GCS@FZJ, Germany. (v) J.H.W.'s research was funded by the Deutsche Forschungsgemeinschaft (DFG, German Research Foundation) - Projektnummer 417533893/GRK2575 "Rethinking Quantum Field Theory". (vi) O.K. acknowledges support by the Deutsche Forschungsgemeinschaft (DFG, German Research Foundation) through the CRC-TR 211 'Strong-interaction matter under extreme conditions'– project number 315477589 – TRR 211.

References

[1] T. Matsui and H. Satz, *J/ψ Suppression by Quark-Gluon Plasma Formation*, *Phys. Lett. B* **178** (1986) 416.

[2] G.S. Bali, *QCD forces and heavy quark bound states*, *Phys. Rept.* **343** (2001) 1.

[3] TUMQCD collaboration, *Determination of the QCD coupling from the static energy and the free energy*, *Phys. Rev. D* **100** (2019) 114511.

[4] A. Rothkopf, T. Hatsuda and S. Sasaki, *Proper heavy-quark potential from a spectral decomposition of the thermal Wilson loop*, *PoS* **LAT2009** (2009) 162.

[5] Y. Burnier and A. Rothkopf, *A hard thermal loop benchmark for the extraction of the nonperturbative $Q\bar{Q}$ potential*, *Phys. Rev. D* **87** (2013) 114019.

[6] M. Laine, O. Philipsen, P. Romatschke and M. Tassler, *Real-time static potential in hot QCD*, *JHEP* **03** (2007) 054.

[7] A. Hasenfratz and F. Knechtli, *Flavor symmetry and the static potential with hypercubic blocking*, *Phys. Rev. D* **64** (2001) 034504 [hep-lat/0103029].

[8] M. Lüscher, *Properties and uses of the Wilson flow in lattice QCD*, *JHEP* **08** (2010) 071 [1006.4518].

[9] M. Luscher and P. Weisz, *Perturbative analysis of the gradient flow in non-abelian gauge theories*, *JHEP* **02** (2011) 051 [1101.0963].

[10] D. Hoying, A. Bazavov, D. Bala, G. Parkar, O. Kaczmarek, R. Larsen et al., *Static potential at non-zero temperatures from fine lattices*, *PoS* **LATTICE2021** (2022) 178 [2110.00565].

[11] HotQCD collaboration, *Static quark-antiquark interactions at nonzero temperature from lattice QCD*, *Phys. Rev. D* **105** (2022) 054513.

[12] R. Larsen, S. Meinel, S. Mukherjee and P. Petreczky, *Excited bottomonia in quark-gluon plasma from lattice QCD*, *Phys. Lett. B* **800** (2020) 135119.

[13] L. Schlessinger, *Use of analyticity in the calculation of nonrelativistic scattering amplitudes*, *Phys. Rev.* **167** (1968) 1411.

[14] Y. Burnier and A. Rothkopf, *Bayesian Approach to Spectral Function Reconstruction for Euclidean Quantum Field Theories*, *Phys. Rev. Lett.* **111** (2013) 182003.

[15] D. Bala and S. Datta, *Nonperturbative potential for the study of quarkonia in QGP*, *Phys. Rev. D* **101** (2020) 034507.

[16] L. Mazur, *Topological aspects in lattice QCD*, Ph.D. thesis, Ph. D. thesis, Bielefeld University, 2021.

[17] D. Bollweg et al., *HotQCD on multi-GPU Systems*, *PoS* **LATTICE2021** (2022) 196.

[18] A. Ramos and S. Sint, *Symanzik improvement of the gradient flow in lattice gauge theories*, *Eur. Phys. J. C* **76** (2016) 15 [1508.05552].

[19] Y. Burnier and A. Rothkopf, *Complex heavy-quark potential and Debye mass in a gluonic medium from lattice QCD*, *Phys. Rev. D* **95** (2017) 054511.

[20] Y. Burnier, O. Kaczmarek and A. Rothkopf, *Static quark-antiquark potential in the quark-gluon plasma from lattice QCD*, *Phys. Rev. Lett.* **114** (2015) 082001.